11 as a rapid preequilibrium. On the basis of the literature value[27]

$$k_{II} = k_3 K_a(Ti^{3+})/[H^+] \quad (13)$$

for $K_a(Ti^{3+})$, k_3 was calculated as 4.25 ± 0.13 M^{-1} s^{-1} at I = 1.0 (LiCl) and 25 °C.

The rate constant for the reaction of perhydroxyl with titanyl must be on the order of 2×10^3 M^{-1} s^{-1} (see above). Thus, a free enthalpy of activation of ~0.56 eV is estimated to reach the transition state $[(TiO\cdots HO_2^{\bullet})^{2+}]^{\ddagger}$. A different transition state is formed by the oxidation of $TiOH^{2+}$ with O_2. This reaction exhibits a free energy of activation of 0.72 eV, and furthermore, $TiOH^{2+}$ and O_2 are less stable than TiO^{2+} and $HO_2^{\bullet}$ by 0.23 eV. Therefore, the energy of the transition state $[(TiOH\cdots O_2)^{2+}]^{\ddagger}$ lies 0.95 eV above the TiO^{2+} + $HO_2^{\bullet}$ level. The transition state $[(TiOH\cdots O_2)^{2+}]^{\ddagger}$ is less stable than $[(TiO\cdots HO_2^{\bullet})^{2+}]^{\ddagger}$ by ~0.39 eV and arises either from outer-sphere electron transfer or from oxygen addition to $TiOH^{2+}$, which would lead to $Ti(OH)(O_2^{\bullet})^{2+}$ as a primary product. This shows that $Ti(OH)(O_2^{\bullet})^{2+}$ is less stable than $TiO(HO_2^{\bullet})^{2+}$.

(27) Orhanović, M.; Earley, J. E. *Inorg. Chem.* **1975**, *14*, 1478.

The stability constant for perhydroxytitanyl(2+) formation, $K_{HO_2\bullet} \approx k_{-1}/k_{1,0}$ is estimated as ~8.4×10^4 M^{-1} and the reduction potential of $TiO(HO_2^{\bullet})^{2+}$ as ~1.35 V. We were unable to oxidize $Ti(O_2)^{2+}$ by cyclic voltammetry in 0.1-1.0 M $HClO_4$ using a SnO_2 or a glassy-carbon electrode, presumably because the electron transfer at the electrode is too slow.

The $TiO(HO_2^{\bullet})^{2+}$ ion is a slightly weaker oxidizing agent than the free $HO_2^{\bullet}$ radical, but in contrast to the case for free $HO_2^{\bullet}$, it is most likely a much poorer reducing agent, since molecular oxygen coordinated to TiO^{2+} would be formed as an unstable product. Probably for this reason, dismutation of perhydroxytitanyl(2+), reaction 14, is too slow to be observed in competition with reactions 4 and 5.

$$2TiO(HO_2^{\bullet})^{2+} \rightarrow Ti(O_2)^{2+} + TiO(O_2)^{2+} + H_2O \quad (14)$$

Acknowledgment. P. Compte recorded the CV's. Professor Dr. R. C. Thompson, Dr. E. Müller, and Dr. R. Humphry-Baker contributed helpful comments on the manuscript. The work was supported by the National Energy Research Foundation.

Registry No. $Ti(O_2)^{2+}$, 12179-34-9; $TiO(HO_2^{\bullet})^{2+}$, 110487-74-6; $TiOH^{2+}$, 21029-47-0.

Contribution from the Department of Chemistry, University of South Carolina, Columbia, South Carolina 29208

Cluster Synthesis. 15. Square-Pyramidal Coordination of Sulfur in Metal Cluster Complexes. Synthesis and Structural Characterizations of $Ru_4(CO)_7(\mu\text{-}CO)_2(PMe_2Ph)_2(\mu_4\text{-}S)(\mu_5\text{-}S)[W(CO)_4PMe_2Ph]$ and $Os_5(CO)_{15}(\mu_5\text{-}S)[W(CO)_4PPh_3]$

Richard D. Adams,* James E. Babin, K. Natarajan, Miklos Tasi, and Jin-Guu Wang

Received April 14, 1987

The compounds $Ru_4(CO)_7(\mu\text{-}CO)_2(PMe_2Ph)_2(\mu_4\text{-}S)(\mu_5\text{-}S)[W(CO)_4PMe_2Ph]$ (**2**) and $Os_5(CO)_{15}(\mu_5\text{-}S)[W(CO)_4PPh_3]$ (**4**) have been obtained in yields of 40% and 35% by the irradiation of solutions containing $W(CO)_5(PMe_2Ph)$ and $Ru_4(CO)_9(PMe_2Ph)_2(\mu_4\text{-}S)_2$ and solutions containing $W(CO)_5(PPh_3)$ and $Os_5(CO)_{15}(\mu_4\text{-}S)$, respectively. Both products were characterized by X-ray diffraction analyses. For **2**: space group $P2_1/c$, a = 12.408 (2) Å, b = 29.353 (7) Å, c = 13.903 (2) Å, β = 111.69 (1)°, V = 4705 (2) Å^3, Z = 4. For **4**: space group $P2_1/c$, a = 19.839 (9) Å, b = 16.461 (6) Å, c = 27.407 (10) Å, β = 92.94 (3)°, V = 8939 (7) Å^3, Z = 8. Both products contain pentacoordinate, square-pyramidal, quintuply bridging sulfido ligands formed by the addition of a $W(CO)_4PR_3$ group to a quadruply bridging sulfido ligand of the original complex. The W-S bond lengths of 2.486 (2) Å in **2** and 2.52 (2) Å in **4** are not significantly different from those for W-S bonds to tetravalent sulfido ligands. The attachment of the tungsten-containing group to the sulfido ligand does not produce any significant structural changes upon the bonding of the sulfido ligand to the clusters in either case.

Introduction

The strong affinity of sulfur for the elements of the transition series serves as a basis for a variety of important naturally occurring metal sulfur compounds. Metal sulfides constitute the most important class of mineral ores.[1] Metal–sulfur complexes play a central role in the activity of a variety of biologically important enzymes and coenzymes.[2] Metal–sulfur compounds have been shown to have an enormous commercial value as hydrodesulfurization catalysts.[3]

Recent studies of metal complexes have shown that the coordination chemistry of sulfur is extremely rich and varied.[4] Sulfido ligands commonly exhibit doubly (A), triply (B), and quadruply (C and D) bridging bonding modes. The ligand is remarkably flexible. M–S–M bond angles may be as small as 65° or as large as 140°.[5] A recent report of an "inverted" tetrahedral coordination E, demonstrates how extreme these distortions may become.[6] The only known examples of pentacoordinate sulfur exist in an unusual class of metal-rich minerals known as pentlandites.[7]

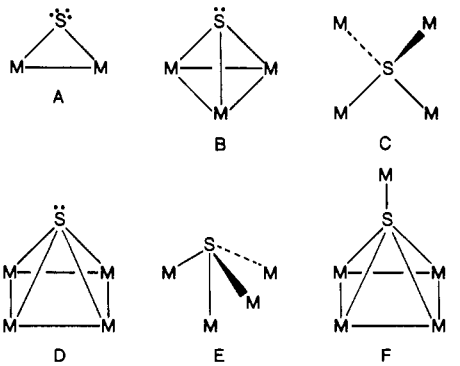

(1) Vaughn, D. J.; Craig, J. R. *Mineral Chemistry of Metal Sulfides*; Cambridge University Press: Cambridge, U.K., 1978.
(2) (a) Coughlin, M. P., Ed., *Molybdenum and Molybdenum Containing Enzymes*; Pergamon: Oxford U.K., 1980. (b) Lovenberg, W., Ed. *Iron Sulfur Proteins*; Academic: New York, 1976.
(3) Schuman, S. C.; Shalit, H. *Catal. Rev.* **1970**, *4*, 245.
(4) Vahrenkamp, H. *Angew. Chem., Int. Ed. Engl.* **1975**, *14*, 322.
(5) Adams, R. D.; Foust, D. F. *Organometallics* **1983**, *2*, 323.
(6) Adams, R. D.; Hor, T. S. A. *Organometallics* **1984**, *3*, 1915.

0020-1669/87/1326-3708$01.50/0

In these materials a square-pyramidal arrangement of metal atoms surrounds the sulfur atom (F).

In the quadruply bridging mode D, the sulfido ligand is believed to serve as a four-electron donor.[4,8] Thus, it should contain a lone pair of electrons. However, the Lewis basicity of this ligand has not heretofore been demonstrated. In this report we describe the nature of the addition of unsaturated metal carbonyl moieties to complexes that contain quadruply bridging sulfido ligands D. These products show that the attachment occurs on the sulfido ligand. They demonstrate the Lewis basicity of the quadruply bridging sulfido ligand and show for the first time that pentacoordination F is a viable and perhaps important mode of bonding for sulfur in molecular metal complexes. A preliminary report of part of this study has been published.[9]

Experimental Section

Although the reagents and products are air stable, all reactions were performed under a dry nitrogen atmosphere. Reagent grade solvents were dried over molecular sieves and were deoxygenated with N_2 prior to use. PMe_2Ph and PPh_3 were purchased from Aldrich and were used without further purification. Photolysis experiments were performed by using an external high-pressure mercury lamp on reaction solutions contained in Pyrex glassware. IR spectra were recorded on a Nicolet 5-DXB FT-IR spectrophotometer. ^1H NMR spectra were run on a Bruker AM-300 spectrometer operating at 300 MHz. $W(CO)_6$ was purchased from Strem Chemicals, Newburyport, MA, and was sublimed before use. $W(CO)_5(PMe_2Ph)$,[10] $W(CO)_5(PPh_3)$,[10] $Ru_4(CO)_9(PMe_2Ph)_2(\mu_4\text{-}S)_2$ (**1**),[11] and $Os_5(CO)_{15}(\mu_4\text{-}S)$ (**3**)[12] were prepared by published procedures.

Preparation of $Ru_4(CO)_9(\mu_4\text{-}S)(\mu_5\text{-}S)(PMe_2Ph)_2[W(CO)_4PMe_2Ph]$ (2). A 37-mg (0.08-mmol) sample of $W(CO)_5PMe_2Ph$ was dissolved in 50 mL of hexane and was photolyzed for 75 min. under a continuous purge with N_2. During this period a solution of 17 mg (0.017 mmol) of $Ru_4(CO)_9(\mu_4\text{-}S)_2(PMe_2Ph)_2$ (**1**) in 10 mL of hexane was added dropwise to the solution of $W(CO)_5PMe_2Ph$. After the addition was completed, the reaction solution was photolyzed for an additional 45 min. The solvent was removed in vacuo, and the residue was dissolved in a minimum amount of CH_2Cl_2 and was chromatographed by TLC on silica gel by using a 3/2 hexane/CH_2Cl_2 (v/v) solvent mixture as eluent. This yielded the following compounds in order of elution: 7 mg of orange unreacted **1**; 1.3 mg of a light orange compound that has not been fully characterized yet [IR (ν(CO) in hexane, cm^{-1}): 2016 (vs), 1991 (m), 1949 (m), 1939 (vs), 1902 (vw), 1852 (vw), 1811 (vw)]; and 5.7 mg of dark brown $Ru_4(CO)_9(\mu_4\text{-}S)(PMe_2Ph)_2(\mu_5\text{-}S)[W(CO)_4PMe_2Ph]$ (**2**) in 40% yield based on the amount of **1** consumed. IR (ν(CO) in hexane, cm^{-1}) 2047 (w), 2022 (vs), 2012 (m), 2001 (m), 1967 (m), 1888 (s), 1850 (vw), 1810 (vw). ^1H NMR (δ in C_6D_6): 7.10–6.80 (m, 15 H), 1.22 (d, $J_{P\text{-}H}$ = 10 Hz, 12 H), 1.18 (d, $J_{P\text{-}H}$ = 8 Hz, 6 H).

Preparation of $Os_5(CO)_{15}(\mu_5\text{-}S)[W(CO)_4(PPh_3)]$ (4). $Os_5(CO)_{15}(\mu_4\text{-}S)$ (**3**) (30 mg 0.0121 mmol) was dissolved in 100 mL of hexane solvent. $W(CO)_5(PPh_3)$ (25 mg 0.043 mmol) was added, and the solution was irradiated under a continuous N_2 purge for 3 h. The solvent was removed in vacuo, and the residue was chromatographed by TLC on silica gel with a 20%/80% CH_2Cl_2/hexane solvent mixture. This yielded an orange band of unreacted **3** (8 mg) and a red band, **4** (10.5 mg, 35%). IR for **4** (ν(CO) in hexane, cm^{-1}): 2105 (vw), 2091 (w), 2067 (vs), 2056 (m), 2045 (m), 2031 (s), 2013 (m), 2002 (w), 1996 (wv,sh), 1899 (m). ^1H NMR (δ in $CDCl_3$): 7.43 (m).

Crystallographic Analyses. Dark brown crystals of **2** were grown from solutions in CH_2Cl_2/hexane/benzene solvent mixtures by cooling to 0 °C. Red-orange platelets of **4** were grown by slow evaporation of a solution in a CH_2Cl_2/hexane solvent mixture at −20 °C. Diffraction measurements for **2** were made on a Rigaku AFC6 fully automated four-circle diffractometer. Intensity measurements for **4** were collected on an Enraf-Nonius CAD4 X-ray diffractometer at the Molecular Structure Corp., College Station, TX. Structure solutions and refinements for **2** and **4** were performed on a Digital Equipment Corp. MICROVAX II computer by using Molecular Structure Corporation's TEXSAN program library and on a VAX 11/782 computer by using the Enraf-Nonius program library SDP-PLUS, respectively. Unit cells were determined by using the automatic search, center, index, and least-squares routines of the diffractometers. Crystal data and structure refinement results are listed in Table I. Neutral-atom scattering factors and anomalous dispersion coefficients were calculated by the standard procedures.[13] Full-matrix least-squares refinements minimized the function

$$\sum_{hkl} w(|F_o| - |F_c|)^2$$

Table I. Crystallographic Data for the Structural Analyses for Compounds **2** and **4**

	2	**4**
	(A) Crystal Data	
formula	$Ru_4WS_2P_2O_{13}C_{37}H_{33}$	$Os_5WSPO_{19}C_{13}H_{15}$
temp, °C (±3)	23	23
space group	$P2_1/c$	$P2_1/c$
a, Å	12.408 (2)	19.839 (9)
b, Å	29.353 (7)	16.461 (6)
c, Å	13.903 (2)	27.407 (10)
α, deg	90.0	90.0
β, deg	111.69 (1)	92.94 (3)
γ, deg	90.0	90.0
V, Å^3	4705 (2)	8939 (7)
M_r	1430.8	1961.4
Z	4	8
ρ_{calcd}, g/cm^3	2.02	2.92
	(B) Measurement of Intensity Data	
radiation	Mo Kα (0.71073 Å)	Mo Kα (0.71073 Å)
monochromator	graphite	graphite
detector aperture, mm		
horiz	2.0	2.0
vert	2.0	2.0
cryst faces	011, 0$\bar{1}\bar{1}$, 1$\bar{1}$0 $\bar{1}$00, 01$\bar{1}$, 0$\bar{1}$1	001, 00$\bar{1}$, 010, 0$\bar{1}$0, $\bar{1}$10, 1$\bar{1}$0
cryst size, mm	0.13 × 0.20 × 0.27	0.03 × 0.07 × 0.35
cryst orientation: direction; deg from ϕ axis	[120]; 18	[011]; 0.5
reflcns measd	$h,k,\pm l$	$h,k,\pm l$
max 2θ, deg	48°	40°
scan type	moving cryst–stationary counter	moving cryst–moving counter
ω-scan width (A + 0.347 tan θ), deg	1.10	0.7
bkgd	$^1/_4$ addtl scan at each end of scan	$^1/_4$ addtl scan at each end of scan
ω-scan rate, deg/min	4.0[a]	variable, 4–20
no. of reflcns measd (unique)	7573	8744
no. of data used ($F^2 \geq 3.0\sigma(F^2)$)	5658	3354
	(C) Treatment of Data	
abs cor	applied	applied
coeff, cm^{-1}	40.5	169.5
grid	empirical	14 × 10 × 8
transmissn coeff		
max	1.00	0.60
min	0.69	0.33
P factor	0.02	0.04
final residuals		
R_F	0.028	0.047
R_{wF}	0.028	0.055
esd of unit wt observn	1.25	1.65
largest shift/error value of final cycle	0.07	0.13
largest peak in final diff Fourier, e/Å^3	0.79	0.13
no. of variables	541	573

[a] Rigaku software uses a multiple scan technique. If the $I/\sigma(I)$ ratio is less than 10.0, a second scan is made and the results are added to first scan, etc. A maximum of three scans was permitted per reflection.

(7) (a) Rajamani, V.; Prewitt, C. T. *Can. Mineral.* **1973**, *12*, 178. (b) Hall, S. R.; Stewart, J. M. *Can. Mineral.* **1973**, *12*, 169.
(8) Adams, R. D. *Polyhedron* **1985**, *4*, 2003.
(9) Adams, R. D.; Babin, J. E.; Natarajan, K. *J. Am. Chem. Soc.* **1986**, *108*, 3518.
(10) Mathieu, R.; Lenzi, M.; Poilblanc, R. *Inorg. Chem.* **1970**, *9*, 2030.
(11) Adams, R. D.; Babin, J. E.; Tasi, M. *Inorg. Chem.* **1986**, *25*, 4514.
(12) Adams, R. D.; Horvath, I. T. H.; Segmuller, B. E.; Yang, L. *Organometallics* **1983**, *2*, 1301.
(13) *International Tables for X-ray Crystallography*, Kynoch: Birmingham, England, 1975; Vol. IV, Table 2.2B, pp 99–101, and Table 2.3.1, pp 149–150.

Table II. Positional Parameters and B(eq) for $Ru_4(CO)_7(\mu\text{-}CO)_2(\mu_4\text{-}S)(\mu_5\text{-}S)[W(CO)_4PMe_2Ph]$ (**2**)

atom	x	y	z	B(eq), Å^2
W	0.72712 (2)	0.09520 (1)	0.39660 (2)	2.51 (1)
Ru(1)	0.94347 (4)	0.10572 (2)	0.20423 (4)	2.33 (2)
Ru(2)	0.81746 (4)	0.18383 (2)	0.18523 (4)	2.40 (2)
Ru(3)	0.74743 (4)	0.05990 (2)	0.08820 (4)	2.65 (2)
Ru(4)	0.61239 (4)	0.13921 (2)	0.06569 (4)	2.34 (2)
S(1)	0.7512 (1)	0.11013 (5)	0.2296 (1)	2.30 (6)
S(2)	0.7944 (1)	0.13434 (5)	0.0356 (1)	2.58 (6)
P(1)	1.0955 (1)	0.10631 (6)	0.1461 (1)	3.04 (7)
P(2)	0.5150 (1)	0.15139 (6)	−0.1086 (1)	2.97 (7)
P(3)	0.7028 (1)	0.08738 (6)	0.5609 (1)	3.01 (7)
O(11)	1.0906 (4)	0.0666 (2)	0.4093 (4)	5.3 (3)
O(12)	1.0706 (4)	0.1896 (2)	0.3238 (4)	4.2 (2)
O(13)	0.9643 (5)	0.0027 (2)	0.1666 (5)	5.5 (3)
O(21)	0.8486 (6)	0.2710 (2)	0.0858 (5)	7.0 (3)
O(22)	0.8068 (5)	0.2444 (2)	0.3555 (5)	6.0 (3)
O(31)	0.7118 (6)	0.0140 (2)	−0.1147 (5)	7.8 (3)
O(32)	0.6138 (6)	−0.0143 (2)	0.1415 (6)	9.0 (4)
O(41)	0.5364 (5)	0.2314 (2)	0.1095 (5)	6.3 (3)
O(42)	0.4049 (5)	0.0912 (2)	0.0780 (5)	7.2 (3)
O(51)	0.5730 (5)	0.1837 (2)	0.3397 (5)	6.8 (3)
O(52)	0.9635 (5)	0.1475 (2)	0.5082 (5)	6.2 (3)
O(53)	0.4990 (5)	0.0360 (2)	0.3065 (5)	6.7 (3)
O(54)	0.8615 (6)	0.0027 (2)	0.4077 (5)	7.4 (3)
C(1)	1.2216 (6)	0.0748 (3)	0.2248 (7)	5.2 (4)
C(2)	1.0575 (7)	0.0815 (3)	0.0191 (6)	5.1 (4)
C(3)	0.5606 (7)	0.2055 (3)	−0.1530 (6)	5.4 (4)
C(4)	0.5397 (6)	0.1082 (3)	−0.1897 (5)	4.6 (4)
C(5)	0.7941 (7)	0.1212 (3)	0.6686 (6)	5.4 (4)
C(6)	0.7264 (7)	0.0315 (3)	0.6207 (6)	4.8 (4)
C(11)	1.0366 (6)	0.0820 (2)	0.3318 (6)	3.2 (3)
C(12)	0.9908 (6)	0.1706 (2)	0.2656 (5)	2.7 (3)
C(13)	0.9109 (6)	0.0357 (2)	0.1548 (6)	3.5 (3)
C(21)	0.8383 (7)	0.2376 (3)	0.1230 (6)	4.1 (3)
C(22)	0.8087 (6)	0.2203 (2)	0.2910 (6)	3.7 (3)
C(31)	0.7245 (7)	0.0311 (3)	−0.0386 (6)	4.3 (3)
C(32)	0.6667 (7)	0.0133 (3)	0.1221 (7)	4.8 (4)
C(41)	0.5720 (6)	0.1972 (3)	0.0967 (6)	4.2 (3)
C(42)	0.4824 (6)	0.1096 (3)	0.0724 (5)	3.8 (3)
C(51)	0.6321 (6)	0.1519 (3)	0.3654 (6)	4.1 (3)
C(52)	0.8765 (6)	0.1290 (2)	0.4675 (5)	3.3 (3)
C(53)	0.5810 (7)	0.0581 (3)	0.3356 (5)	3.9 (3)
C(54)	0.8152 (6)	0.0367 (3)	0.4084 (6)	4.1 (3)

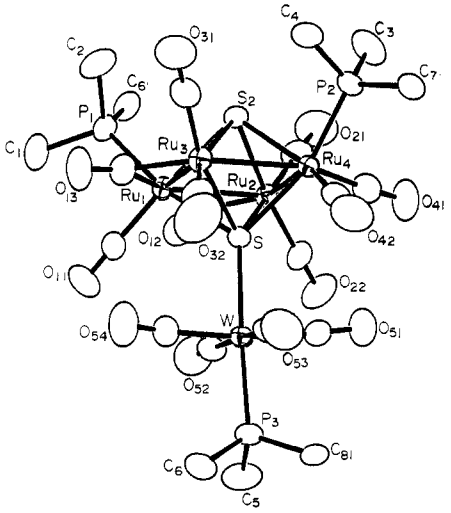

Figure 1. ORTEP diagram of $Ru_4(CO)_7(\mu\text{-}CO)_2(PMe_2Ph)_2(\mu_4\text{-}S)(\mu_5\text{-}S)[W(CO)_4PMe_2Ph]$ (**2**) showing 50% probability thermal ellipsoids.

where $w = 1/\sigma(F_o)^2$, $\sigma(F) = \sigma(F_o^2)/2F_o$, and $\sigma(F_o^2) = [\sigma(I_{raw})^2 + (PF_o^2)^2]^{1/2}/Lp$. The structure of **2** was obtained by a combination of direct methods (MITHRIL) and difference Fourier syntheses. The positions of the hydrogen atoms were calculated and were included in the structure factor calculations. The structure of **4** was solved by a combination of direct methods (MULTAN) and difference Fourier techniques. The hydrogen atoms were ignored in the analysis of **4**. A table of observed and calculated structure factor amplitudes for **4** has been deposited.[9]

Table III. Selected Intramolecular Bond Distances (Å) for $Ru_4(CO)_7(\mu\text{-}CO)_2(PMe_2Ph)_2(\mu_4\text{-}S)(\mu_5\text{-}S)[W(CO)_4PMe_2Ph]$ (**2**)

W–C(51)	1.993 (7)	Ru(4)–C(41)	1.871 (8)
W–C(52)	2.010 (7)	Ru(4)–P(2)	2.302 (2)
W–C(54)	2.011 (7)	Ru(4)–S(1)	2.447 (2)
W–C(53)	2.013 (8)	Ru(4)–S(2)	2.449 (2)
W–P(3)	2.424 (2)	P(1)–C(1)	1.799 (8)
W–S(1)	2.486 (2)	P(1)–C(2)	1.805 (8)
Ru(1)–C(11)	1.857 (7)	P(1)–C(61)	1.814 (7)
Ru(1)–C(12)	2.080 (7)	P(2)–C(3)	1.784 (8)
Ru(1)–C(13)	2.157 (7)	P(2)–C(4)	1.797 (8)
Ru(1)–P(1)	2.310 (2)	P(2)–C(71)	1.800 (7)
Ru(1)–S(2)	2.534 (2)	P(3)–C(5)	1.805 (8)
Ru(1)–S(1)	2.541 (2)	P(3)–C(6)	1.814 (8)
Ru(1)–Ru(3)	2.7255 (8)	P(3)–C(81)	1.823 (7)
Ru(1)–Ru(2)	2.7325 (8)	O(11)–C(11)	1.132 (8)
Ru(2)–C(22)	1.854 (7)	O(12)–C(12)	1.164 (7)
Ru(2)–C(21)	1.863 (8)	O(13)–C(13)	1.150 (8)
Ru(2)–C(12)	2.061 (6)	O(21)–C(21)	1.138 (8)
Ru(2)–S(2)	2.466 (2)	O(22)–C(22)	1.149 (8)
Ru(2)–S(1)	2.473 (2)	O(31)–C(31)	1.129 (8)
Ru(2)–Ru(4)	2.7976 (9)	O(32)–C(32)	1.138 (8)
Ru(3)–C(32)	1.856 (8)	O(41)–C(41)	1.136 (8)
Ru(3)–C(31)	1.879 (8)	O(42)–C(42)	1.130 (8)
Ru(3)–C(13)	2.021 (7)	O(51)–C(51)	1.159 (8)
Ru(3)–S(2)	2.443 (2)	O(52)–C(52)	1.152 (8)
Ru(3)–S(1)	2.444 (2)	O(53)–C(53)	1.147 (8)
Ru(3)–Ru(4)	2.8173 (8)	O(54)–C(54)	1.152 (8)
Ru(4)–C(42)	1.865 (7)		

Table IV. Intramolecular Bond Angles (deg) for $Ru_4(CO)_7(\mu\text{-}CO)_2(PMe_2Ph)_2(\mu_4\text{-}S)(\mu_5\text{-}S)[W(CO)_4(PMe_2Ph)]$ (**2**)

C(51)–W–C(52)	93.3 (3)	S(2)–Ru(3)–Ru(1)	58.40 (4)
C(51)–W–C(54)	172.7 (3)	S(2)–Ru(3)–Ru(4)	54.93 (4)
C(51)–W–C(53)	89.5 (3)	S(1)–Ru(3)–Ru(1)	58.58 (4)
C(51)–W–P(3)	90.8 (2)	S(1)–Ru(3)–Ru(4)	54.88 (4)
C(51)–W–S(1)	85.1 (2)	Ru(1)–Ru(3)–Ru(4)	91.26 (3)
C(52)–W–C(54)	90.4 (3)	P(2)–Ru(4)–S(1)	161.80 (6)
C(52)–W–C(53)	175.4 (3)	P(2)–Ru(4)–S(2)	89.30 (6)
C(52)–W–P(3)	89.9 (2)	P(2)–Ru(4)–Ru(2)	124.14 (5)
C(52)–W–S(1)	87.9 (2)	P(2)–Ru(4)–Ru(3)	107.74 (5)
C(54)–W–C(53)	87.1 (3)	S(1)–Ru(4)–S(2)	76.29 (5)
C(54)–W–P(3)	95.5 (2)	S(1)–Ru(4)–Ru(2)	55.78 (4)
C(54)–W–S(1)	88.7 (2)	S(1)–Ru(4)–Ru(3)	54.79 (4)
C(53)–W–P(3)	86.5 (2)	S(2)–Ru(4)–Ru(2)	55.60 (4)
C(53)–W–S(1)	95.8 (2)	S(2)–Ru(4)–Ru(3)	54.73 (4)
P(3)–W–S(1)	175.28 (6)	Ru(2)–Ru(4)–Ru(3)	87.02 (2)
P(1)–Ru(1)–S(2)	94.86 (6)	Ru(3)–S(1)–Ru(4)	70.34 (5)
P(1)–Ru(1)–S(1)	167.99 (6)	Ru(3)–S(1)–Ru(2)	103.66 (6)
P(1)–Ru(1)–Ru(3)	117.52 (5)	Ru(3)–S(1)–W	132.20 (7)
P(1)–Ru(1)–Ru(2)	118.16 (5)	Ru(3)–S(1)–Ru(1)	66.24 (4)
S(2)–Ru(1)–S(1)	73.15 (5)	Ru(4)–S(1)–Ru(2)	69.31 (4)
S(2)–Ru(1)–Ru(3)	55.21 (4)	Ru(4)–S(1)–W	130.19 (6)
S(2)–Ru(1)–Ru(2)	55.70 (4)	Ru(4)–S(1)–Ru(1)	105.18 (6)
S(1)–Ru(1)–Ru(3)	55.17 (4)	Ru(2)–S(1)–W	123.57 (6)
S(1)–Ru(1)–Ru(2)	55.78 (4)	Ru(2)–S(1)–Ru(1)	66.03 (4)
Ru(3)–Ru(1)–Ru(2)	90.19 (3)	W–S(1)–Ru(1)	124.30 (6)
S(2)–Ru(2)–S(1)	75.51 (5)	Ru(3)–S(2)–Ru(4)	70.34 (4)
S(2)–Ru(2)–Ru(1)	58.06 (4)	Ru(3)–S(2)–Ru(2)	103.90 (6)
S(2)–Ru(2)–Ru(4)	55.01 (4)	Ru(3)–S(2)–Ru(1)	66.39 (4)
S(1)–Ru(2)–Ru(1)	58.19 (4)	Ru(4)–S(2)–Ru(2)	69.39 (4)
S(1)–Ru(2)–Ru(4)	54.91 (4)	Ru(4)–S(2)–Ru(1)	105.37 (6)
Ru(1)–Ru(2)–Ru(4)	91.54 (3)	Ru(2)–S(2)–Ru(1)	66.24 (4)
S(2)–Ru(3)–S(1)	76.45 (5)		

Results

$W(CO)_5(PMe_2Ph)$ reacts with $Ru_4(CO)_9(PMe_2Ph)_2(\mu_4\text{-}S)_2$ (**1**) in the presence of UV irradiation to give the product $Ru_4(CO)_7(\mu\text{-}CO)_2(PMe_2Ph)_2(\mu_4\text{-}S)(\mu_5\text{-}S)[W(CO)_4(PMe_2Ph)]$ (**2**) in 40% yield. Compound **2** was characterized by IR, ^{1}H, NMR, and a single-crystal X-ray diffraction analysis.

An ORTEP drawing of the molecular structure of **2** is shown in Figure 1. Positional parameters are listed in Table II. Selected intramolecular bond distances and angles are listed in Tables III and IV, respectively. The molecule can be viewed as a combination of two fragments: (1) a unit of $Ru_4(CO)_7(\mu\text{-}CO)_2(PMe_2Ph)_2(\mu_4\text{-}S)_2$ and (2) a $W(CO)_4(PMe_2Ph)$ fragment that is linked to

Table V. Positional and Thermal Parameters (Isotropic) with Esd's for $Os_5(CO)_{15}(\mu_5\text{-}S)[W(CO)_4(PPh_3)]$ (**4**)

atom	*x*	*y*	*z*	*B*, Å^2	atom	*x*	*y*	*z*	*B*, Å^2
Os(1A)	0.6809 (1)	0.1137 (1)	0.18568 (9)	2.48 (5)	O(16B)	0.781 (2)	−0.220 (3)	0.336 (2)	9 (1)[a]
Os(1B)	0.8383 (1)	−0.6193 (1)	0.20251 (9)	2.89 (6)	O(16A)	0.717 (2)	−0.243 (3)	0.079 (2)	8 (1)[a]
Os(2A)	0.5780 (1)	0.0689 (1)	0.11537 (8)	2.29 (5)	O(17B)	0.798 (2)	−0.343 (2)	0.484 (2)	7 (1)[a]
Os(2B)	0.8869 (1)	−0.5704 (1)	0.39755 (8)	2.98 (6)	O(17A)	0.535 (2)	−0.109 (2)	0.012 (1)	5 (1)[a]
Os(3A)	0.7107 (1)	0.0024 (1)	0.10916 (8)	2.33 (5)	O(18B)	1.010 (2)	−0.401 (2)	0.467 (2)	6 (1)[a]
Os(3B)	0.7622 (1)	−0.5108 (1)	0.35732 (9)	3.13 (6)	O(18A)	0.582 (2)	−0.287 (3)	0.208 (2)	7 (1)[a]
Os(4A)	0.7072 (1)	−0.0545 (1)	0.20616 (8)	2.59 (5)	O(19A)	0.421 (2)	−0.155 (2)	0.137 (1)	4.8 (9)[a]
Os(4B)	0.8286 (1)	−0.4490 (1)	0.27665 (9)	3.64 (6)	O(19B)	1.004 (2)	−0.257 (3)	0.322 (2)	8 (1)[a]
Os(5A)	0.5755 (1)	0.0079 (1)	0.21236 (8)	2.70 (5)	C(18)	0.899 (3)	−0.707 (3)	0.297 (2)	5 (1)[a]
Os(5B)	0.9530 (1)	−0.5158 (1)	0.31381 (9)	3.58 (6)	C(1A)	0.690 (3)	0.191 (4)	0.144 (2)	5 (2)[a]
W(1A)	0.5704 (1)	−0.2000 (1)	0.10687 (8)	2.20 (5)	C(2B)	0.773 (3)	−0.689 (4)	0.326 (2)	6 (2)[a]
W(1B)	0.9004 (1)	−0.3033 (1)	0.40266 (9)	2.49 (6)	C(2A)	0.635 (3)	0.177 (3)	0.220 (2)	5 (2)[a]
S(1A)	0.6143 (6)	−0.0677 (8)	0.1424 (5)	1.9 (3)[a]	C(3B)	0.812 (4)	−0.640 (5)	0.242 (3)	11 (3)[a]
S(1B)	0.8721 (6)	−0.4364 (8)	0.3611 (4)	1.6 (3)[a]	C(3A)	0.750 (3)	0.125 (4)	0.234 (2)	6 (2)[a]
P(1A)	0.5403 (7)	−0.3289 (8)	0.0662 (5)	2.6 (3)[a]	C(4B)	0.862 (3)	−0.675 (3)	0.414 (2)	3 (1)[a]
P(1B)	0.9361 (7)	−0.1755 (8)	0.4427 (5)	2.4 (3)[a]	C(4A)	0.488 (3)	0.032 (3)	0.093 (2)	3 (1)[a]
O(1A)	0.714 (2)	0.254 (3)	0.119 (2)	8 (1)[a]	C(5B)	0.980 (3)	−0.583 (4)	0.415 (3)	7 (2)[a]
O(1B)	0.927 (3)	−0.767 (3)	0.300 (2)	11 (2)[a]	C(5A)	0.599 (3)	0.101 (3)	0.057 (2)	5 (2)[a]
O(2A)	0.606 (2)	0.234 (3)	0.244 (2)	8 (1)[a]	C(6B)	0.876 (3)	−0.536 (3)	0.462 (2)	5 (2)[a]
O(2B)	0.729 (2)	−0.736 (3)	0.337 (2)	9 (1)[a]	C(6A)	0.541 (3)	0.174 (3)	0.125 (2)	3 (1)[a]
O(3A)	0.804 (3)	0.146 (3)	0.248 (2)	10 (2)[a]	C(7B)	0.688 (3)	−0.544 (3)	0.315 (2)	4 (1)[a]
O(3B)	0.784 (4)	−0.664 (5)	0.200 (3)	19 (3)[a]	C(7A)	0.786 (3)	−0.070 (3)	0.112 (2)	4 (1)[a]
O(4B)	0.851 (2)	−0.742 (2)	0.429 (1)	5 (1)[a]	C(8B)	0.735 (2)	−0.570 (3)	0.410 (2)	3 (1)[a]
O(4A)	0.441 (2)	0.003 (2)	0.079 (1)	6 (1)[a]	C(8A)	0.761 (3)	0.085 (4)	0.087 (2)	7 (2)[a]
O(5B)	1.037 (2)	−0.597 (2)	0.432 (2)	6 (1)[a]	C(9B)	0.711 (3)	−0.420 (3)	0.381 (2)	3 (1)[a]
O(5A)	0.612 (2)	0.126 (2)	0.016 (1)	5 (1)[a]	C(9A)	0.695 (3)	−0.030 (3)	0.044 (2)	5 (2)[a]
O(6B)	0.857 (2)	−0.509 (2)	0.499 (1)	4.0 (8)[a]	C(10B)	0.873 (4)	−0.354 (4)	0.255 (3)	8 (2)[a]
O(6A)	0.518 (2)	0.239 (3)	0.134 (2)	7 (1)[a]	C(10A)	0.737 (3)	−0.163 (3)	0.197 (2)	5 (1)[a]
O(7A)	0.833 (2)	−0.107 (2)	0.115 (1)	5 (1)[a]	C(11B)	0.742 (3)	−0.404 (4)	0.279 (2)	6 (2)[a]
O(7B)	0.645 (2)	−0.563 (2)	0.289 (1)	5 (1)[a]	C(11A)	0.795 (3)	−0.033 (3)	0.218 (2)	3 (1)[a]
O(8B)	0.715 (2)	−0.614 (2)	0.442 (1)	5 (1)[a]	C(12A)	0.690 (4)	−0.067 (4)	0.264 (3)	8 (2)[a]
O(8A)	0.797 (2)	0.130 (3)	0.069 (2)	8 (1)[a]	C(12B)	0.808 (5)	−0.469 (6)	0.213 (4)	14 (3)[a]
O(9B)	0.683 (2)	−0.368 (2)	0.394 (1)	6 (1)[a]	C(13B)	0.955 (3)	−0.498 (4)	0.255 (2)	5 (1)[a]
O(9A)	0.679 (2)	−0.055 (2)	0.004 (1)	3.8 (8)[a]	C(13A)	0.585 (3)	0.053 (4)	0.272 (2)	6 (2)[a]
O(10B)	0.890 (2)	−0.293 (3)	0.247 (2)	9 (1)[a]	C(14B)	1.012 (3)	−0.613 (4)	0.309 (2)	6 (2)[a]
O(10A)	0.749 (2)	−0.235 (2)	0.195 (2)	6 (1)[a]	C(14A)	0.535 (3)	−0.086 (3)	0.236 (2)	4 (1)[a]
O(11A)	0.858 (2)	−0.021 (2)	0.226 (1)	6 (1)[a]	C(15B)	1.028 (3)	−0.463 (4)	0.346 (2)	6 (2)[a]
O(11B)	0.700 (3)	−0.354 (3)	0.269 (2)	10 (1)[a]	C(15A)	0.493 (3)	0.053 (4)	0.205 (2)	6 (2)[a]
O(12A)	0.682 (2)	−0.086 (3)	0.310 (2)	7 (1)[a]	C(16B)	0.822 (3)	−0.254 (3)	0.361 (2)	4 (1)[a]
O(12B)	0.805 (3)	−0.489 (4)	0.174 (2)	12 (2)[a]	C(16A)	0.661 (3)	−0.223 (3)	0.084 (2)	5 (2)[a]
O(13B)	0.990 (2)	−0.467 (3)	0.218 (2)	9 (1)[a]	C(17B)	0.835 (3)	−0.330 (4)	0.455 (2)	6 (2)[a]
O(13A)	0.598 (2)	0.085 (3)	0.311 (2)	8 (1)[a]	C(17A)	0.557 (3)	−0.145 (3)	0.050 (2)	5 (1)[a]
O(14B)	1.053 (2)	−0.660 (3)	0.307 (2)	8 (1)[a]	C(18B)	0.971 (3)	−0.366 (3)	0.444 (2)	5 (1)[a]
O(14A)	0.510 (2)	−0.145 (2)	0.252 (2)	6 (1)[a]	C(18A)	0.578 (3)	−0.249 (4)	0.167 (2)	6 (2)[a]
O(15A)	0.439 (2)	0.084 (3)	0.200 (2)	8 (1)[a]	C(19B)	0.965 (3)	−0.277 (3)	0.355 (2)	4 (1)[a]
O(15B)	1.071 (3)	−0.424 (3)	0.356 (2)	11 (2)[a]	C(19A)	0.475 (3)	−0.171 (4)	0.127 (2)	6 (2)[a]

[a] Isotropic *B*.

the Ru_4 cluster by an S→W donor–acceptor bond from one of the quadruply bridging sulfido ligands. The Ru_4 cluster unit of **2** is remarkably similar to that in the free molecule **1**. In both cases the Ru_4 unit contains two carbonyl ligands that bridge adjacent edges of the cluster. The metal–metal bonds that are bridged by these ligands are significantly shorter (approximately 0.1 Å) than the others. The contraction of these bonds may be due to the bridging CO ligands but may also be influenced by the electronic unsaturation of the cluster.[11] Atom S(1) forms a coordinate bond to the tungsten atom and is therefore a quintuple (pentacoordinate) bridge. The W–S bond distance of 2.486 (2) Å is slightly shorter than the W–S distance of 2.522 (8) Å observed for a W–S coordinate bond between a $W(CO)_5$ fragment and a triply bridging sulfido ligand in the complex $Os_3(CO)_9(\mu_3\text{-}S)(\mu_4\text{-}S)[W(CO)_5]$ (**5**)[14] and 2.547 (6) Å to a similarly coordinated $W(CO)_5$ group in the compound $Fe_3(CO)_9(\mu_3\text{-}P\text{-}t\text{-}Bu)(\mu_4\text{-}S)[W(CO)_5]$ (**6**).[15] Interestingly, there are no significant differences in the Ru–S distances between the quadruply bridging sulfido ligand S(2) and quintuple bridge S(1). Both sulfido ligands are displaced 1.51 Å from the Ru_4 plane. An interesting difference between **1** and the Ru_4 cluster in **2** is the disposition of the two phosphine ligands. In **1** the phosphine ligands lie on opposite sides of the Ru_4 plane. In **2** they lie on the same side and away from the $W(CO)_4PMe_2Ph$ group. This arrangement clearly results in reduced steric interactions. The six-coordinate tungsten atom has approximately octahedral geometry with all four carbonyl ligands lying in a plane. The S(1)–W–P(3) angle of 175.28 (6)° is slightly nonlinear. This group is rotated 40° with respect to the Ru_4 square in order to minimize the steric interactions between the terminal carbonyl ligands C(11)–O(11), C(22)–O(22), C(32)–O(32), and C(42)–O(42) on the cluster and the carbonyl groups on the tungsten atom.

$W(CO)_5(PPh_3)$ reacts with $Os_5(CO)_{15}(\mu_4\text{-}S)$ (**3**) in the presence of UV irradiation to give the product $Os_5(CO)_{15}(\mu_5\text{-}S)[W(CO)_4PPh_3]$ (**4**) in 35% yield. Compound **4** crystallizes with two independent molecules in the asymmetric crystal unit. Both molecules are structurally similar, and an ORTEP diagram of one of these is shown in Figure 2. Positional parameters are listed in Table V. Selected intramolecular bond distances and angles are listed in Tables VI and VII. As with **2**, compound **4** can be viewed as a combination of two groups: (1) an $Os_5(CO)_{15}(\mu_4\text{-}S)$ cluster complex and (2) a $W(CO)_4PPh_3$ fragment. The latter is linked to the cluster via a S → W donor–acceptor bond. The metal–metal and metal–sulfur bonding in the Os_5S cluster in **4** is nearly identical with that in the free molecule **3**.[12] In both compounds the sulfur atom is displaced 1.42 Å from the base of the cluster. The tungsten–sulfur bond [2.52 (2) Å] is slightly longer than that in **2** but is similar to those in **5** and **6**. The coordination geometry about the tungsten atom is approximately

(14) Adams, R. D.; Horvath, I. T.; Wang, S. *Inorg. Chem.* **1985**, *24*, 1728.
(15) Winter, A.; Jibril, I.; Huttner, G. *J. Organomet. Chem.* **1983**, *242*, 259.

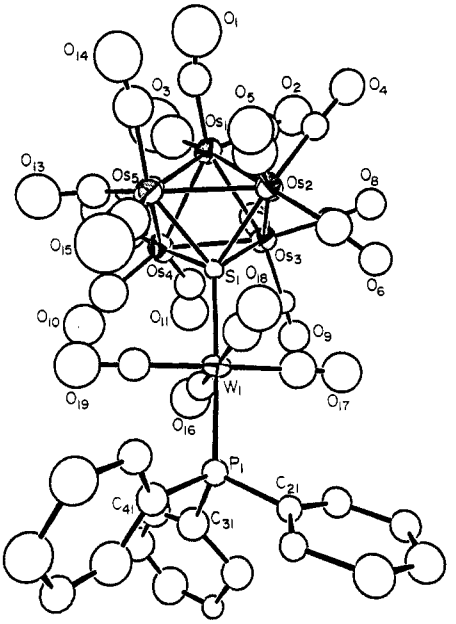

Figure 2. ORTEP diagram of one of the two crystallographically independent molecules of $Os_5(CO)_{15}(\mu_5\text{-}S)[W(CO)_4(PPh_3)]$ (**4**) showing 50% probability thermal ellipsoids.

Table VI. Selected Interatomic Distances (Å) with Esd's for $Os_5(CO)_{15}(\mu_5\text{-}S)[W(CO)_4(PPh_3)]$ (**4**)

molecule A		molecule B	
Os(1A)–Os(2A)	2.831 (3)	Os(1B)–Os(2B)	2.847 (3)
Os(1A)–Os(3A)	2.869 (3)	Os(1B)–Os(3B)	2.822 (3)
Os(1A)–Os(4A)	2.868 (3)	Os(1B)–Os(4B)	2.895 (3)
Os(1A)–Os(5A)	2.844 (3)	Os(1B)–Os(5B)	2.845 (3)
Os(1A)–C(1A)	1.73 (5)	Os(1B)–C(1B)	1.89 (5)
Os(1A)–C(2A)	1.70 (5)	Os(1B)–C(2B)	1.88 (6)
Os(1A)–C(3A)	1.88 (6)	Os(1B)–C(3B)	1.76 (9)
Os(2A)–Os(3A)	2.863 (2)	Os(2B)–Os(3B)	2.831 (3)
Os(2A)–Os(5A)	2.844 (3)	Os(2B)–Os(5B)	2.846 (3)
Os(2A)–C(1A)	2.46 (1)	Os(2B)–C(1B)	2.43 (2)
Os(2A)–C(4A)	1.96 (5)	Os(2B)–C(4B)	1.86 (5)
Os(2A)–C(5A)	1.76 (5)	Os(2B)–C(5B)	1.91 (7)
Os(2A)–C(6A)	1.91 (5)	Os(2B)–C(6B)	1.87 (5)
Os(3A)–Os(4A)	2.823 (3)	Os(3B)–Os(4B)	2.822 (3)
Os(3A)–S(1A)	2.45 (2)	Os(3B)–S(1B)	2.50 (2)
Os(3A)–C(7A)	1.90 (5)	Os(3B)–C(7B)	1.92 (5)
Os(3A)–C(8A)	1.82 (6)	Os(3B)–C(8B)	1.84 (5)
Os(3A)–C(9A)	1.88 (5)	Os(3B)–C(9B)	1.93 (5)
Os(4A)–Os(5A)	2.822 (3)	Os(4B)–Os(5B)	2.842 (3)
Os(4A)–S(1A)	2.48 (2)	Os(4B)–S(1B)	2.44 (2)
Os(4A)–C(10A)	1.90 (6)	Os(4B)–C(10B)	1.91 (7)
Os(4A)–C(11A)	1.80 (5)	Os(4B)–C(11B)	1.88 (6)
Os(4A)–C(12A)	1.65 (7)	Os(4B)–C(12B)	1.8 (1)
Os(5A)–S(1A)	2.44 (2)	Os(5B)–S(1B)	2.49 (2)
Os(5A)–C(13A)	1.80 (6)	Os(5B)–C(13B)	1.66 (5)
Os(5A)–C(14A)	1.88 (5)	Os(5B)–C(14B)	2.00 (6)
Os(5A)–C(15A)	1.80 (6)	Os(5B)–C(15B)	1.91 (6)
W(1A)–S(1A)	2.52 (2)	W(1B)–S(1B)	2.52 (2)
W(1A)–P(1A)	2.46 (1)	W(1B)–P(1B)	2.47 (1)
W(1A)–C(16A)	1.97 (5)	W(1B)–C(16B)	2.05 (5)
W(1A)–C(17A)	1.81 (5)	W(1B)–C(17B)	2.03 (6)
W(1A)–C(18A)	1.83 (6)	W(1B)–C(18B)	2.05 (5)
W(1A)–C(19A)	2.06 (6)	W(1B)–C(19B)	1.93 (6)

octahedral with four linear carbonyl ligands lying in a plane. The $W(CO)_4$ group is rotated (28°) relative to the Os_4 square in order to minimize the steric interactions between the carbonyl ligands on the cluster and those on the tungsten atom. Interestingly, the CO ligands attached to the metal atoms on the Os_4 square in **4** are arranged to form an approximate fourfold rotational symmetry about this unit. This is significantly different from that in **3** and is probably induced by the steric interactions with the $W(CO)_4$ group, which contains a similar fourfold symmetry. The S–W–P angle is 172.8 (4)° [176.1 (4)°].[16]

Table VII. Selected Interatomic Angles (deg) with Esd's for $Os_5(CO)_{15}(\mu_5\text{-}S)[W(CO)_4PPh_3]$ (**4**)

molecule A		molecule B	
Os(2A)–Os(1A)–Os(3A)	60.31 (6)	Os(2B)–Os(1B)–Os(3B)	59.93 (7)
Os(2A)–Os(1A)–Os(4A)	90.00 (7)	Os(2B)–Os(1B)–Os(4B)	88.01 (7)
Os(2A)–Os(1A)–Os(5A)	60.17 (7)	Os(2B)–Os(1B)–Os(5B)	60.02 (7)
Os(3A)–Os(1A)–Os(4A)	58.96 (7)	Os(3B)–Os(1B)–Os(4B)	59.13 (7)
Os(3A)–Os(1A)–Os(5A)	88.80 (7)	Os(3B)–Os(1B)–Os(5B)	90.59 (7)
Os(4A)–Os(1A)–Os(5A)	59.19 (6)	Os(4B)–Os(1B)–Os(5B)	59.35 (7)
Os(1A)–Os(2A)–Os(3A)	60.50 (6)	Os(1B)–Os(2B)–Os(3B)	59.59 (7)
Os(1A)–Os(2A)–Os(5A)	60.16 (7)	Os(1B)–Os(2B)–Os(5B)	59.97 (7)
Os(1A)–Os(2A)–S(1A)	81.0 (3)	Os(1B)–Os(2B)–S(1B)	81.5 (2)
Os(3A)–Os(2A)–Os(5A)	88.90 (7)	Os(3B)–Os(2B)–Os(5B)	90.37 (9)
Os(3A)–Os(2A)–S(1A)	54.1 (2)	Os(3B)–Os(2B)–S(1B)	56.1 (2)
Os(5A)–Os(2A)–S(1A)	54.2 (2)	Os(5B)–Os(2B)–(1B)	55.5 (2)
Os(1A)–Os(3A)–Os(2A)	59.19 (6)	Os(1B)–Os(3B)–Os(2B)	60.47 (7)
Os(1A)–Os(3A)–Os(4A)	60.51 (7)	Os(1B)–Os(3B)–Os(4B)	61.73 (7)
Os(1A)–Os(3A)–S(1A)	80.5 (3)	Os(1B)–Os(3B)–S(1B)	80.9 (2)
Os(2A)–Os(3A)–Os(4A)	90.25 (7)	Os(2B)–Os(3B)–Os(4B)	89.77 (8)
Os(2A)–Os(3A)–S(1A)	54.6 (3)	Os(2B)–Os(3B)–S(1B)	53.9 (2)
Os(4A)–Os(3A)–S(1A)	55.7 (3)	Os(4B)–Os(3B)–S(1B)	54.1 (2)
Os(1A)–Os(4A)–Os(3A)	60.53 (7)	Os(1B)–Os(4B)–Os(3B)	59.15 (7)
Os(1A)–Os(4A)–Os(5A)	59.98 (7)	Os(1B)–Os(4B)–Os(5B)	59.46 (7)
Os(1A)–Os(4A)–S(1A)	79.9 (3)	Os(1B)–Os(4B)–S(1B)	80.5 (3)
Os(3A)–Os(4A)–Os(5A)	90.16 (8)	Os(3B)–Os(4B)–Os(5B)	90.67 (8)
Os(3A)–Os(4A)–S(1A)	54.5 (2)	Os(3B)–Os(4B)–S(1B)	56.2 (2)
Os(5A)–Os(4A)–S(1A)	54.4 (2)	Os(5B)–Os(4B)–S(1B)	55.5 (2)
Os(1A)–Os(5A)–Os(2A)	59.69 (7)	Os(1B)–Os(5B)–Os(2B)	60.02 (7)
Os(1A)–Os(5A)–Os(4A)	60.83 (6)	Os(1B)–Os(5B)–Os(4B)	61.19 (7)
Os(1A)–Os(5A)–S(1A)	81.1 (3)	Os(1B)–Os(5B)–S(1B)	80.7 (2)
Os(2A)–Os(5A)–Os(4A)	90.67 (7)	Os(2B)–Os(5B)–Os(4B)	89.05 (8)
Os(2A)–Os(5A)–S(1A)	54.9 (3)	Os(2B)–Os(5B)–S(1B)	53.8 (2)
Os(4A)–Os(5A)–S(1A)	55.8 (2)	Os(4B)–Os(5B)–S(1B)	54.0 (2)
S(1A)–W(1A)–P(1A)	172.8 (4)	S(1B)–W(1B)–P(1B)	176.1 (4)
Os(2A)–S(1A)–Os(3A)	71.3 (3)	Os(2B)–S(1B)–Os(3B)	70.1 (3)
Os(2A)–S(1A)–Os(4A)	109.1 (4)	Os(2B)–S(1B)–Os(4B)	110.0 (4)
Os(2A)–S(1A)–Os(5A)	70.9 (3)	Os(2B)–S(1B)–Os(5B)	70.7 (3)
Os(2A)–S(1A)–W(1A,	125.6 (4)	Os(2B)–S(1B)–W(1B)	125.7 (4)
Os(3A)–S(1A)–Os(4A)	69.8 (3)	Os(3B)–S(1B)–Os(4B)	69.7 (3)
Os(3A)–S(1A)–Os(5A)	109.6 (4)	Os(3B)–S(1B)–Os(5B)	107.8 (4)
Os(3A)–S(1A)–W(1A)	121.6 (4)	Os(3B)–S(1B)–W(1B)	128.8 (4)
Os(4A)–S(1A)–Os(5A,	69.9 (3)	Os(4B)–S(1B)–Os(5B)	70.5 (3)
Os(4A)–S(1A)–W(1A)	125.2 (4)	Os(4B)–S(1B)–W(1B)	124.3 (4)
Os(5A)–S(1A)–W(1A)	128.8 (4)	Os(5B)–S(1B)–W(1B)	124.0 (4)

Discussion

Compounds **1** and **3** each consist of clusters of metal atoms and have at least one quadruply bridging sulfido ligand across a square of four metal atoms. A (phosphine)tungsten tetracarbonyl moiety produced by an irradiation-induced decarbonylation of the parent pentacarbonyl compound was added to each of the complexes **1** and **3** through the formation of a sulfur to tungsten donor–acceptor bond. As a result, the quadruply bridging sulfido ligands have become pentacoordinate and exhibit a square-pyramidal coordination geometry. A comparison of the structures of **1** with **2** and **3** with **4** shows that the attachment of the tungsten-containing group to the sulfido ligand has no significant structural effect on the bonding of the sulfido ligand to the cluster.

The pentacoordinate sulfido ligand, presumably, utilizes all six of its valence electrons in bonding (i.e., two electrons are donated to the tungsten atom and four are donated to the cluster). Although square-pyramidal coordination generally implies the involvement of five atomic orbitals (e.g., sp^3d), according to the most popular delocalized bonding theories, this would not be necessary in these examples since the bonding of the sulfido ligand to the square of four metal atoms would require the use of only three atomic orbtials.[17]

The results reported here demonstrate the intrinsic stability of pentacoordinate sulfur in molecular complexes. The ability of the quadruply bridging ligand D to expand its coordination by the addition of a metal atom suggests that the quadruply bridging sulfido ligand could also be useful as a focal point for the aggregation of metal atoms and as an aid for cluster synthesis.[8,18]

(16) The quantity in brackets corresponds to the second independent molecule in the crystal.

(17) (a) Wade, K. In *Transition Metal Clusters*; Johnson, B. F. G., Ed.; Wiley: New York, 1980. (b) Johnson, B. F. G.; Benfield, R. E. In *Topics in Stereochemistry*; Geoffroy, G. L., Ed.; Wiley: New York, 1981; Vol. 12.

Acknowledgment. This research was supported by the National Science Foundation under Grant No. CHE-8612862. We wish to thank Johnson-Matthey for a generous loan of osmium tetraoxide. The AM-300 NMR spectrometer was purchased with funds from the National Science Foundation, Grant No. CHE-8411172.

Supplementary Material Available: Listings of hydrogen atom parameters for **2**, anisotropic thermal parameters (U values) for **2** and **4**, and positional parameters of the phenyl ring carbon atoms for **2** and **4** (8 pages); a listing of calculated and observed structure factor amplitudes for **2** (38 pages). A listing of calculated and observed structure factors for **4** was deposited earlier.[9] Ordering information is given on any current masthead page.

(18) Rauchfuss, T. B.; Weatherill, T. B.; Wilson, S. R.; Zebrowski, J. P. *J. Am. Chem. Soc.* **1983**, *105*, 6508.

Contribution from the Departamento Quimica de Reactores, Comisiôn Nacional de Energia Atômica, (1429) Buenos Aires, Argentina

Mechanism of Dissolution of Magnetite by Oxalic Acid–Ferrous Ion Solutions

Miguel A. Blesa,* Horacio A. Marinovich, Erwin C. Baumgartner, and Alberto J. G. Maroto

Received October 21, 1986

The kinetics of the reductive dissolution of magnetite by ferrous ions in solutions of high oxalate concentration has been studied at 30 °C and various pH values. The rate-determining step is proposed to be the outer-sphere electron transfer from $Fe^{II}(C_2O_4)_2^{2-}$, located in the Stern plane, to a surface oxalate–iron(III) complex. Analysis of the work term and electron-transfer Gibbs energy shows that $Fe^{II}(C_2O_4)_2^{2-}$ is a reasonable choice for the reductant species. Dissolution also requires protonation of the surface sites, in a process described by a Freundlich-type isotherm.

Introduction

Oxalic acid is a reagent of choice in many iron oxide solvent formulations.[1] Only a few mechanistic studies are available for these dissolution processes: Sellers and Williams[2] have carried out a study of the dissolution of nickel chromium ferrites by oxalic acid solutions in the temperature range 105–160 °C, and concluded that the mechanism involves the reduction of surface Fe^{III} ions by oxalate, which yields CO_2. Thus, the mechanism is similar to the one proposed earlier for the dissolution of magnetite by thioglycolic acid.[3,4] Further examples of dissolution by reducing complexing anions involve thiocyanate and iodide.[5]

In the case of the dissolution of magnetite by oxalic acid, our own preliminary results[6,7] demonstrated that the process is autocatalytic, the mechanism involving an interfacial electron transfer between ferrous–oxalate complexes and surface ferric ions; the main reaction does not involve the oxidation of oxalate and thus differs significantly from the system studied by Sellers. Indeed, the induction period is related to the reduction of Fe^{III} by oxalate, but the ensuing fast reaction corresponds to the stoichiometry

$$Fe_3O_4 + 8HC_2O_4^- \rightarrow 2Fe(C_2O_4)_3^{3-} + Fe(C_2O_4)_2^{2-} + 4H_2O \quad (1)$$

Of course, in the presence of light, $Fe(C_2O_4)_3^{3-}$ in bulk evolves to $Fe^{II} + CO_2$; analogous species on the surface are photosensitive in a similar way.[5,8]

The electron-transfer process involved in this system was proposed to be an outer-sphere transfer from ferrous complexes to a ferric surface complex[6,7] and is thus mechanistically related to the reductive dissolution of nickel ferrite by vanadous picolinate.[9]

In the present paper we report a detailed kinetic study of this system showing that electron transfer controls the overall rate; this result is at variance with usual assumptions in the field of electrochemistry, where electron transfer is assumed to be fast and controlled by solution redox potential.[10,11] As we were mainly interested in characterizing the outer-sphere reaction, the measurements were carried out in large excess of oxalic acid. As discussed below, both the surface and the reductant were fully complexed, thus preventing the possibility of bridged intermediates that might operate in certain homogeneous electron-transfer reactions mediated by oxalate.[12] Such bridged systems can in fact be also conducive to metal oxide dissolution; this subject shall be analyzed in forthcoming papers on the dissolution of magnetite by nitrilotriacetic (NTA) and ethylenediaminetetraacetic acids (EDTA).[13,14]

Experimental Section

Reagents were of analytical purity or better and were used without further purification. Magnetite was prepared by oxidation of a slurry of ferrous hydroxide with potassium nitrate in the presence of hydrazine.[15] The slurry was obtained by adding ammonia to a $FeCl_2 \cdot 4H_2O$ solution at boiling temperature. The prepared material was found to be a nearly stoichiometric magnetite composed of cuboctahedral particles, modal edge ca. 0.1 μm, as characterized by X-ray powder diffractograms, scanning electron microscopy, and Mössbauer spectroscopy. Its specific surface was measured on a Micromeritics surface analyzer by nitrogen adsorption and BET procedures, a value of 9.7 $m^2\ g^{-1}$ being obtained.

Kinetic experiments were carried out in a cylindrical beaker, surrounded by a water jacket. Suspensions containing 40 mg of magnetite

(1) (a) Blesa, M. A.; Maroto, A. J. G. In *Decontamination of Nuclear Facilities, Keynote Addresses*; American Nuclear Society: Niagara Falls, NY, 1982; p 1. (b) *Decontamination of Nuclear Reactors and Equipment*; Ayres, J. A., Ed.; Ronald Press: New York, 1970. (c) *Decontamination and Decommissioning of Nuclear Facilities*; Osterhout, M., Ed.; Plenum: New York, 1980.
(2) Sellers, R. M.; Williams, W. J. *Faraday Discuss. Chem. Soc.* **1984**, *77*, 265.
(3) Baumgartner, E. C.; Blesa, M. A.; Maroto, A. J. G. *J. Chem. Soc., Dalton Trans.* **1982**, 1649.
(4) Blesa, M. A.; Maroto, A. J. G., Morando, P. J. *J. Chem. Soc., Faraday Trans. 1* **1986**, *82*, 2345.
(5) Blesa, M. A.; Bruyere, V. I. E.; Maroto, A. J. G.; Regazzoni, A. E. *An. Asoc. Quim. Argent.* **1985**, *73*, 39.
(6) Baumgartner, E. C.; Blesa, M. A.; Marinovich, H.; Maroto, A. J. G. *Inorg. Chem.* **1983**, *22*, 2224.
(7) Blesa, M. A.; Maroto, A. J. G. In *Reactivity of Solids*; Barret, P., Dufour, L. C., Eds.; Materials Science Monographs; Elsevier: Amsterdam, 1985; Vol. 28A, p 529.
(8) Waite, T. D.; Morel, F. M. M. *J. Colloid Interface Sci.* **1984**, *102*, 121.
(9) Segal, M. G.; Sellers, R. M. *J. Chem. Soc., Faraday Trans. 1* **1982**, *78*, 1149.
(10) Gorichev, I. G.; Kipriayanov, N. A. *Russ. J. Phys. Chem.* (*Engl. Transl.*) **1981**, *55*, 1558.
(11) Mouhandess, M. T.; Sharara, Z. Z.; Chassagneux, F.; Durand, B.; Vittori, O. In *Reactivity of Solids*; Barret, P., Dufour, L. C., Eds.; Materials Science Monographs; Elsevier: Amsterdam, 1985; Vol. 28A, p 549.
(12) Pennington, D. E. In *Coordination Chemistry*; Martell, A. E., Ed.; ACS Monograph 174; American Chemical Society: Washington, DC, 1978.
(13) Hidalgo, M. d. V.; Katz, N. E.; Blesa, M. A.; Maroto, A. J. G. *J. Chem. Soc., Faraday Trans. 1*, in press.
(14) Borghi, E. B.; Regazzoni, A. E.; Blesa, M. A., unpublished results.
(15) Regazzoni, A. E.; Urrutia, G. A.; Blesa, M. A.; Maroto, A. J. G. *J. Inorg. Nucl. Chem.* **1981**, *43*, 1489.

0020-1669/87/1326-3713$01.50/0